Journal of Cerebral Blood Flow & Metabolism (2005) 25, 807–819

www.jcbfm.com

PET studies of net blood–brain clearance of FDOPA to human brain: age-dependent decline of [^{18}F]fluorodopamine storage capacity

Yoshitaka Kumakura[1,2], Ingo Vernaleken[3], Gerhard Gründer[4], Peter Bartenstein[5], Albert Gjedde[1,2] and Paul Cumming[1,2]

[1]*PET Centre, Aarhus University Hospitals, Aarhus, Denmark;* [2]*Centre for Functionally Integrated Neuroscience, Aarhus, Denmark;* [3]*Department of Psychiatry, University of Mainz, Mainz, Germany;* [4]*Department of Psychiatry and Psychotherapy, University of Aachen, Aachen, Germany;* [5]*Department of Nuclear Medicine, University of Mainz, Mainz, Germany*

Conventional methods for the graphical analysis of 6-[^{18}F]fluorodopa (FDOPA)/positron emission tomography (PET) recordings (K_{in}^{app}) may be prone to negative bias because of oversubtraction of the precursor pool in the region of interest, and because of diffusion of decarboxylated FDOPA metabolites from the brain. These effects may reduce the sensitivity of FDOPA/PET for the detection of age-related changes in dopamine innervations. To test for these biasing effects, we have used a constrained compartmental analysis to calculate the brain concentrations of the plasma metabolite 3-*O*-methyl-FDOPA (OMFD) during 120 mins of FDOPA circulation in healthy young, healthy elderly, and Parkinson's disease subjects. Calculated brain OMFD concentrations were subtracted frame-by-frame from the dynamic PET recordings, and maps of the FDOPA net influx to brain were calculated assuming irreversible trapping (K^{app}). Comparison of K_{in}^{app} and K^{app} maps revealed a global negative bias in the conventional estimates of FDOPA clearance. The present OMFD subtraction method revealed curvature in plots of K^{app} at early times, making possible the calculation of the corrected net influx (K) and also the rate constant for diffusion of decarboxylated metabolites from the brain (k_{loss}). The effective distribution volume (EDV^2; K/k_{loss}) for FDOPA, an index of dopamine storage capacity in brain, was reduced by 85% in putamen of patients with Parkinson's disease, and by 58% in the healthy elderly relative to the healthy young control subjects. Results of the present study support claims that storage capacity for dopamine in both caudate and putamen is more profoundly impaired in patients with Parkinson's disease than is the capacity for DOPA utilization, calculated by conventional FDOPA net influx plots. The present results furthermore constitute the first demonstration of an abnormality in the cerebral utilization of FDOPA in caudate and putamen as a function of normal aging, which we attribute to loss of vesicular storage capacity.
Journal of Cerebral Blood Flow & Metabolism (2005) **25,** 807–819. doi:10.1038/sj.jcbfm.9600079
Published online 23 February 2005

Keywords: compartmental analysis; [^{18}F]fluorodopa; net influx; parametric mapping; PET

Introduction

Positron emission tomography (PET) has been used to map the uptake and retention in the brain of the levodopa analogue [^{18}F]fluorodopa (FDOPA) after intravenous injection (Garnett *et al*, 1983). The preferential accumulation of radioactivity in the healthy striatum during several hours after labeled levodopa administration is linked to the formation *in situ* of labeled dopamine (Cumming *et al*, 1987*a*, *b*, 1988), and the prolonged retention of decarboxylated radiotracer metabolite within synaptic vesicles (Horne *et al*, 1984; Cumming *et al*, 1988; Deep *et al*, 1997). However, the kinetic analysis of FDOPA retention results in a complex model, which requires reduction to allow useful regression (Gjedde *et al*, 1991; Huang *et al*, 1991). Clinical FDOPA/PET studies are frequently quantified by a linear graphical analysis based on methods for calculating the net influx to the brain of deoxyglucose (Gjedde, 1981, 1982; Patlak *et al*, 1983; Patlak

Correspondence: Dr Y Kumakura, PET Centre, Aarhus University Hospital, Nørrebrogade 44, Aarhus C, DK-8000, Denmark.
E-mail: yoshi@pet.auh.dk
This work was supported by funding from the National Science Foundation, Medical Research Council (Denmark) and the Deutsche Forschungs-gemeinschaft DFG (Ba 1101/2-1).
Received 23 August 2004; revised 23 September 2004; accepted 27 September 2004; published online 23 February 2005

and Blasberg, 1985), in which the net influx K is a macroparameter defined as $K_1k_3/(k_2+k_3)$, where K_1 is the unidirectional blood–brain tracer clearance, k_2 is the clearance rate constant of free tracer from brain, and k_3 is the rate constant of irreversible metabolic trapping in the brain by an enzymatic or binding process (Table 1).

The graphical analysis of FDOPA influx is complicated by the accumulation in the brain of the FDOPA plasma metabolite 3-*O*-methyl-[^{18}F]FDOPA (OMFD), and also by the eventual diffusion of decarboxylated FDOPA metabolites from the brain. In practice, the apparent distribution volume of FDOPA in the brain has been estimated by subtraction of the total radioactivity in a nonbinding reference region; the ratio of this apparent distribution volume in the brain relative to the plasma FDOPA concentration is plotted as a linear function of the normalized arterial FDOPA input (K_{in}^{app}; Gjedde, 1988; Martin *et al*, 1989), generally assuming that the product [^{18}F]fluorodopamine is entirely trapped in brain during the course of the PET recording. However, because of the violation of several model-based assumptions, it remains uncertain how the index K_{in}^{app} relates to the kinetically defined net clearance K.

In clinical FDOPA/PET studies of patients with Parkinson's disease, the magnitude of K_{in}^{app} is substantially reduced in the striatum, especially in the putamen (Snow *et al*, 1990; Bhatt *et al*, 1991; Hoshi *et al*, 1993; Ishikawa *et al*, 1996*a*; Vingerhoets *et al*, 1996; de la Fuente-Fernández *et al*, 2000; Rousset *et al*, 2000), in proportion to the extent of loss of nigrostriatal neurons. However, as stated above, this graphical analysis is complicated by the accumulation in plasma of the brain-penetrating metabolite OMFD, which is formed by the action of catechol-*O*-methyltransferase (COMT) in peripheral tissues (Boyes *et al*, 1986; Melega *et al*, 1991; Cumming *et al*, 1993). The effect of the presence of OMFD in the brain on the physiologic interpretation of K_{in}^{app} has been a matter of debate (Cumming *et al*, 1997; Dhawan *et al*, 1997; Holden *et al*, 1997), and the subject of new PET investigations (Sossi *et al*, 2003). In particular, subtraction of the entire radioactivity measured in the reference tissue, assumed to constitute FDOPA and OMFD, must bias the apparent FDOPA distribution volume in binding regions, since this procedure reduces the tracer distribution volume by the concentration of the precursor pool measured in the nonbinding region. Furthermore, the K_{in}^{app} method is uncorrected for the diffusion of [^{18}F]fluorodopamine metabolites from the brain (Cumming *et al*, 1994), which reduces the slope of K_{in}^{app} plots at late circulation times (Holden *et al*, 1997).

In the present study, we hypothesized that K_{in}^{app}, the conventional approach for calculation of FDOPA utilization in the brain, introduces a two-fold bias in the estimation throughout the brain of K, the intrinsic net blood–brain clearance of FDOPA. To test this claim, we now define specific forms of the net blood–brain clearance of FDOPA (Table 1) for the case in which the contribution of OMFD to total brain radioactivity has been removed mathematically (K^{app}), and for the case (K) in which the influx has also been corrected for loss of decarboxylated FDOPA metabolites by simple diffusion (k_{loss}). To this end, a conventional constrained compartmental model was used to calculate the concentration curve for OMFD in the cerebellum, which was then subtracted frame-by-frame from the dynamic emission recordings, before estimation of the net blood–brain clearance. To test for bias, a systematic comparison of the parametric maps of K_{in}^{app} and K^{app} was made in groups of young and aged normal control subjects and in Parkinson's disease patients.

The magnitude of K_{in}^{app} is reduced by the eventual catabolism of [^{18}F]fluorodopamine to metabolites that diffuse from the brain (k_{loss}), especially when calculated from dynamic emission recordings of long duration (Holden *et al*, 1997; Doudet *et al*, 1998; Cumming *et al*, 2001; Sossi *et al*, 2001, 2002, 2003). The effective distribution volume, an index of the specific binding capacity for FDOPA metabolites in the brain, has been defined as the ratio K_{in}^{app}/k_{loss} (EDV^1; Sossi *et al*, 2001, 2002), and in the present study as the ratio K/k_{loss} (EDV^2). We hypothesized that subtraction of the reference tissue radioactivity obscures the negative deviation of influx plots already present during the first two hours of FDOPA circulation, and also obscures declines in the magnitudes of k_{loss} and effective distribution volume (TACs) as a function of normal aging or Parkinson's disease. To test this hypothesis, we used time–radioactivity curves (TACs) prepared by subtraction of the calculated brain OMFD concentrations to calculate the magnitudes of k_{loss} and EDV^2 in the striatum of groups of healthy young, healthy aged, and Parkinson's disease subjects.

Materials and methods

Scanning Procedures

This study was approved by the Research and Ethics Committees of Aarhus University and the University of Mainz. Fifteen neurologically normal healthy subjects divided into groups less than 50 years of age ($n=7$; 27.6 ± 5.2 years) and greater than 50 years of age ($n=8$; 59.0 ± 7.1 years) and five patients with Parkinson's disease (62.0 ± 8.2 years) were recruited. All subjects provided written informed consent to participate in the PET study. The absence of medical, neurologic (other than Parkinson's disease), and psychiatric history (including alcohol and drug abuse) was assessed by history, review of organ systems, physical examination, routine blood test, urine toxicology, and electrocardiogram. Clinical severity and history of the Parkinson's disease subjects are reported elsewhere (Kumakura *et al*, 2004). The Parkinson's disease patients were all positive to the apomorphine challenge test (Bonuccelli *et al*, 1993), had a Hoehn and Yahr score

of II, and a mean duration of illness of 3.7 ± 1.2 years. The patients were under treatment with levodopa (Sinemet) monotherapy, and had never been exposed to COMT inhibitors, monoamine oxidase (MAO) inhibitors, or dopamine direct agonists.

All subjects were scanned in an overnight fasting condition. Parkinson's disease patients had a pause of routine medication for 3 days before the PET examination. Catheters were placed in an antecubital vein and a radial artery of the nondominant hand. Carbidopa (Merck Sharpe and Dohme) was administered 1 h before the initiation of PET recordings in order to block the decarboxylation of the tracer in peripheral tissues (Cumming *et al*, 1993) at a dose of 150 mg (orally). This dose is conventional for human FDOPA/PET studies, and is less than one half that is frequently used in primate studies (Psylla *et al*, 1997; Yee *et al*, 2001). Subjects reclined on the scanning bed of the ECAT EXACT HR 47 whole body positron emission tomograph (CTI/Siemans, Knoxville, TN, USA) operating in 3-D acquisition mode, with their heads comfortably immobilized using a custom-made head-holder. Recording of a 10-min transmission scan was completed just before the radiotracer injection. Recording of a dynamic emission sequence lasting 120 mins was initiated on intravenous injection of FDOPA (200 MBq). The emission recordings typically consisted of 6×0.5, 7×1, 5×2, 4×5, 5×10, and 1×30 mins frames, for a total of 120 mins. During the emission recording, a series of 40 arterial blood samples were collected at the following intervals after tracer injection: 18×10 secs, 4×0.5 mins, 5×1 mins, 6×5 mins, 5 mins, and 7×10 mins. After centrifugation, the total [^{18}F]-radioactivity concentration in plasma was measured with a well-counter cross-calibrated to the tomograph, and decay-corrected to the time of FDOPA injection. The fractions of untransformed FDOPA and its major plasma metabolite OMFD were determined in 8 selected plasma samples (2.5, 5, 15, 25, 35 60, 90, and 120 mins) by reverse-phase high-performance liquid chromatography (Cumming *et al*, 1993), and the continuous input functions for FDOPA and OMFD were calculated by interpolation of biexponential functions to the measured fractions (Gillings *et al*, 2001). The two arterial input curves were used to calculate the magnitudes of the apparent whole body activity of COMT with respect to FDOPA (k_0, min^{-1}) and the rate constant for the elimination of OMFD from plasma (k_{-1} min^{-1}), an index of renal function (Cumming *et al*, 1993), by nonlinear regression.

Preparation of Brain Time–Radioactivity Curves

The entire dynamic PET sequences, consisting of 28 frames, were realigned and corrected for interframe head motion by frame-wise use of a rigid-body transformation with six degrees of freedom using an MRI-derived 4D-template specific for FDOPA (Reilhac *et al*, 2003; Kumakura *et al*, 2004). After motion correction, individual summed emission images were calculated and registered to the MNI stereotaxic brain, using the affine transformation of the AIR algorithm (Woods *et al*, 1992), fitted to a gray matter MRI template of the MNI average brain (Collins *et al*, 1998; International Consortium for Brain Mapping, ICBM) with its striatum intensity doubled, to emulate radioactivity distribution of the emission images. To make use of VOIs drawn on the MNI stereotaxic brain, the summed dynamic emission sequences after motion correction were resampled into the stereotaxic space using the transformations calculated as mentioned above. TACs were then extracted by binary masking VOIs of the bilateral putamen (9.7 cm^3), bilateral caudate (8.5 cm^3), medial frontal cortex (35.3 cm^3) and cerebellum (48.3 cm^3) contoured at a certain threshold of the statistical probabilistic anatomical map of the MNI average brain.

Subtraction of Brain 3-*O*-Methyl-[^{18}F]FDOPA Radioactivity

The schema describing FDOPA kinetics in brain tissue is presented in Figure 1, and the kinetic and modeling terms are defined in Table 1. This model, which identifies at least six parameters in binding regions and four parameters in a nonbinding reference region, is clearly overspecified, and has therefore been reduced by the use of physiologic constraints (Gjedde *et al*, 1991, 1993; Huang *et al*, 1991; Hoshi *et al*, 1993). In particular, the ratio (q) of

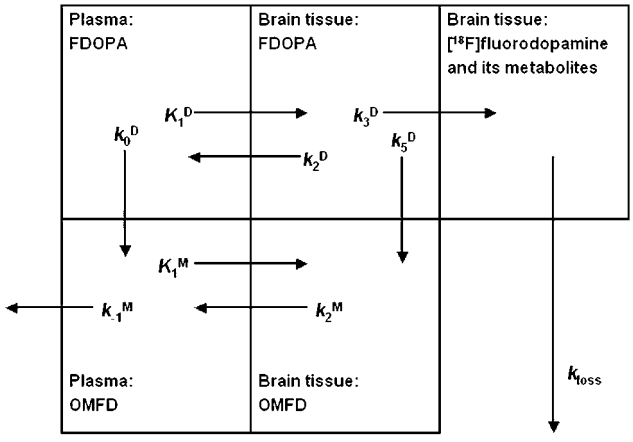

Figure 1 A schema describing [^{18}F]fluorodopa (FDOPA) and 3-*O*-methyl-[^{18}F]FDOPA (OMFD) kinetics in brain tissue. The total radioactivity concentration in a brain region is distributed into three compartments: intravascular space, extravascular tissue (precursor pool), and metabolite compartment (trapped tracer). [^{18}F]fluorodopa in plasma is metabolized by catechol-*O*-methyltransferase at apparent rate constant k_0^D (min^{-1}), and the product OMFD is eliminated from circulation at rate constant k_{-1}^M (min^{-1}). The model defines the unidirectional blood–brain clearances (mL/g min) of FDOPA (K_1^D) and OMFD (K_1^M), and the corresponding rate constants for clearance back to circulation (k_2^D, k_2^M; min^{-1}). The coefficient of brain tissue methylation of FDOPA, k_5^D is assumed to be negligible throughout the brain. The activity of DOPA decarboxylase is assumed to be zero in the cerebellum reference region, but elsewhere FDOPA is decarboxylated at the rate constant k_3^D (min^{-1}). The product [^{18}F]fluorodopamine formed in the brain, together with its subsequent metabolites, is assumed to diffuse from the brain as a single compartment at the rate constant k_{loss} (min^{-1}) (modified after Gjedde *et al*, 1991).

Table 1 Standard kinetic terms used in the text

Term	*Units*	*Definition*
k_0^D	min^{-1}	Whole body *O*-methylation coefficient for plasma FDOPA
k_{-1}^M	min^{-1}	Elimination rate constant for plasma OMFD
K_1	mL/g min	Unidirectional blood–brain clearance of a tracer, K_1^D for the case of FDOPA and K_1^M for the case of OMFD
q	None	The ratio of the blood–brain permeabilities of OMFD and FDOPA (K_1^M/K_1^D), fixed at 1.5 based on several experimental determinations
k_2	min^{-1}	The rate constant for transfer of a tracer in brain to blood
k_3	min^{-1}	The rate constant for the irreversible trapping of a tracer in brain, defined by hexokinase activity in the case of FDG and by the activity of DOPA decarboxylase in the case of FDOPA
V_e	mL/g	The equilibrium distribution volume of a tracer in a nonbinding region (K_1/k_2)
k_3^s (or K^{occ})	min^{-1}	An index of the utilization of FDOPA calculated by graphical analysis using an occipital cortex tissue input
K_{in}^{app}	mL/g min	The net blood–brain clearance of FDOPA in a region of interest calculated by graphical analysis, with subtraction of the total radioactivity measured in a nonbinding region, and assuming no loss of decarboxylated metabolites
K_{in}	mL/g min	The net blood–brain clearance of FDOPA in a region of interest calculated by graphical analysis, with subtraction of the total radioactivity measured in a nonbinding region, and assuming diffusion of decarboxylated metabolites from the brain
K^{app}	mL/g min	The net blood–brain clearance of FDOPA in a region of interest calculated by graphical analysis after mathematical subtraction of the calculated brain concentrations of OMFD, and assuming no loss of decarboxylated metabolites
K	mL/g min	The intrinsic utilization or net blood–brain clearance of a tracer defined kinetically in terms of K_1, k_2, and k_3
k_4	min^{-1}	In the case of FDG, the return of trapped FDG-phosphate to the precursor pool in the brain
k_7	min^{-1}	The activity of monoamine oxidase with respect to [^{18}F]fluorodopamine in the brain
k_9	min^{-1}	The rate constant for the diffusion of acidic [^{18}F]fluorodopamine metabolites from the brain
k_{loss}	min^{-1}	The rate constant for the diffusion of decarboxylated FDOPA metabolites from the brain, a composite of k_7 and k_9
EDV^1	mL/g	The ratio K_{in}^{app}/k_{loss}, an index of the dopamine storage capacity in the brain (Sossi *et al*, 2001)
EDV^2	mL/g	The ratio K/k_{loss}, an index of the dopamine storage capacity in the brain

the unidirectional clearances of OMFD (K_1^M) and FDOPA (K_1^D), was fixed to the mean experimentally determined value of 1.5 (Cumming and Gjedde, 1998), the two amino acids are assumed to have a common blood–brain partition volume ($V_e = K_1^D/k_2^D = K_1^M/k_2^M$), and, in the present analysis, the plasma volume in the brain (V_0) was fixed at 0.05 mL/g (see Cumming and Gjedde (1998) for discussion and experimental support for these assumptions). In the constrained model, the magnitude of V_e is first determined in the cerebellum, where the rate constant for decarboxylation of FDOPA (k_3^D) is assumed to be zero. The estimate of V_e is then used as a constrained input parameter for the estimation of the magnitude of k_3^D in brain regions containing DOPA decarboxylase activity. In the present analysis, the one-compartment constrained model was fitted to the dynamic TACs recorded in the cerebellum during the initial 60 mins of FDOPA circulation. Thus, the parameters to be estimated in the cerebellum by nonlinear optimization were the unidirectional blood–brain clearance (K_1^D) and the elimination rate constant of FDOPA from the brain (k_2^D), calculated using custom-made software on IDL (Research Systems Inc., Boulder, CO, USA). In the course of this optimization procedure, the corresponding estimates of K_1^M and k_2^M in the cerebellum are also obtained by the multiplicative factor q, according to the assumptions of the constrained compartmental model described above. Then, a brain TAC was calculated for OMFD as a convolution of the plasma OMFD input function and the impulse response function determined by K_1^M and k_2^M, assumed to be of uniform magnitude throughout the brain. Finally, the calculated TAC for OMFD in the cerebellum was subtracted frame-by-frame from the original dynamic recording.

To test for age effects in tracer bioavailability, the area under the curve (AUC) for plasma FDOPA of the six youngest (26.0 ± 3.5 years) and six eldest (61.0 ± 7.1 years) normal subjects was calculated during the 120 mins recording interval and normalized to a common FDOPA input with AUC of 500 MBq/mL min. Individual plasma OMFD TACs were then rescaled using the same normalization factor, and the mean normalized OMFD inputs were calculated in groups of the six youngest and six oldest normal control subjects. Individual OMFD curves calculated in the cerebellum in the young and elderly control subjects were normalized to the common FDOPA arterial input.

Mapping of [^{18}F]fluorodopa Influx

Voxel-wise graphical analysis of the magnitude of the net blood–brain clearance of FDOPA (Gjedde, 1981, 1982; Patlak *et al*, 1983; Patlak and Blasberg, 1985) was performed in the PET native space using MATLAB (The Mathworks, Natick, MA, USA). Maps of the net blood–brain clearance, K_{in}^{app}, were calculated by graphical analysis with conventional frame-by-frame subtraction of the total TAC in the cerebellum (Martin *et al*, 1989). Maps of the net clearance were likewise calculated using the dynamic images after frame-by-frame subtraction of the

calculated brain OMFD concentration (K^{app}). For the preceding calculations, the individual metabolite-corrected arterial inputs for FDOPA were used, and the linearization was obtained using emission frames recorded in the interval of 20 to 60 mins, based upon earlier experience (Cumming and Gjedde, 1998). The resultant parametric maps were resampled into the common stereotaxic space using the transformations calculated as described above. The individual K_{in}^{app} and K^{app} maps were smoothed with an isotropic 3-D Gaussian kernel of 12 mm full-width at half-maximum (FWHM), and mean images were calculated for each of the three groups (healthy young, healthy aged, and Parkinson's disease subjects). Effects of the subject group and method of analysis on the mean estimates in the caudate, putamen, and medial frontal cortex were tested using the two-tailed Student's *t*-test.

k_{loss} and Effective Distribution Volume

Based on a generalization of graphical analysis (Patlak and Blasberg, 1985), the conventional method for estimation of K_{in}^{app} has been extended by correcting for the eventual catabolism of [^{18}F]fluorodopamine and diffusion of its acidic metabolites from the brain (k_{loss}; Holden *et al*, 1997; Doudet *et al*, 1998). This method has previously been applied to the analysis of 4-h-long emission recordings; in the present study, we tested methods for the estimation of the magnitudes of K_{in} and k_{loss} using the available 2-h-long recordings. The ratio of the magnitudes of K_{in}^{app} and k_{loss} has previously been defined as the effective distribution volume of FDOPA in the brain (EDV[1]). In the present analysis, we used the modified graphical analysis to estimate the magnitudes in the brain of K and k_{loss} (and the ratio, EDV[2]), that is, after subtraction of the calculated brain OMFD radioactivity, and with exclusion of the first ten minutes of data from the nonlinear regressions of the 2-h-long data sets.

Results

The mean magnitude of K_1^D in the cerebellum was close to 0.03 mL/g in all subject groups (not shown), as reported previously (Cumming and Gjedde, 1998). The mean magnitude of V_e from the compartmental modeling of cerebellum was 0.78 ± 0.17 mL/g for the healthy young population, 0.74 ± 0.09 mL/g for the healthy elderly population, and 0.87 ± 0.06 mL/g for the Parkinson's disease population ($P < 0.05$, compared with the age-matched healthy population).

A typical fitting of the constrained compartmental model to a TAC recorded in the cerebellum and the calculated TAC for OMFD in the brain are illustrated in Figure 2. The measured AUC in the putamen of a normal subject and the curve calculated by subtraction of the calculated brain OMFD curve are shown in Figure 3A, and the linear graphical analyses

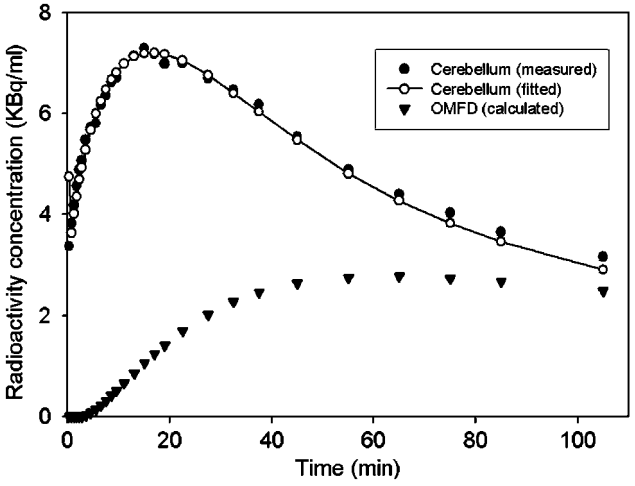

Figure 2 The brain time-radioactivity curve measured in the cerebellum of a normal subject during 120 mins after injection of [^{18}F]fluorodopa (FDOPA), along with the fitting of the constrained compartmental model to the measured data, and the time–radioactivity curve for 3-*O*-methyl-[^{18}F]FDOPA (OMFD) so-calculated.

(Patlak/Gjedde plots) of the same data by the methods of K_{in}^{app} and K^{app} are shown in Figure 3B.

The population-mean rate constants for the formation of OMFD in plasma (k_0^D) and its elimination from plasma (k_{-1}^M) are summarized in Table 2. There was a significant decline in the magnitude of k_{-1}^M with age. For the six youngest and six eldest subjects, the mean normalized plasma input functions for OMFD (Figure 4A) are shown along with the calculated cerebellum concentrations of OMFD (Figure 4B). The mean area under the normalized plasma curves for OMFD was 260 ± 37 MBq/mL min for the six youngest subjects and 374 ± 110 MBq/mL min for the six eldest normal subjects (Figure 4A; $P = 0.036$); the two groups were significantly different at all times after 50 mins ($P < 0.05$). The mean area under the normalized radioactivity concentration curves for OMFD in the cerebellum in the young (197 ± 47 MBq/mL) and in the elderly (230 ± 43 MBq/mL) groups did not differ, although at all times after 50 mins, cerebellum OMFD concentrations were greater in the elderly group ($P < 0.05$, see Figure 4B).

Mean parametric maps of K_{in}^{app} and K^{app} in the healthy young, healthy elderly, and Parkinson's disease patients are illustrated in Figure 5. The mean estimates of K_{in}^{app}, K^{app}, and K in the frontal cortex, caudate, and putamen are summarized in Table 3. Relative to the mean magnitudes of K_{in}^{app}, the magnitudes of K^{app} were significantly higher in all three brain structures for all three subject groups. Throughout the brain, and in all subject groups, the magnitude of K^{app} was positively offset from the magnitude of K_{in}^{app} by 0.0042 ± 0.0016 mL/g in the young subjects, 0.0027 ± 0.0018 mL/g min in the healthy

elderly group, and 0.0028 ± 0.0018 mL/g in the Parkinson's disease group (not significant). Stable estimates of the magnitudes of K_{in} and k_{loss} using the method of Sossi *et al* (2001) could not be obtained using the present 2-h-long emission recordings. However, it was possible to calculate K and k_{loss} in VOIs from the medial frontal cortex, caudate and putamen after frame-by-frame subtraction of the calculated brain OMFD concentrations (Table 3); magnitudes of K were significantly greater than K_{in}^{app} and K^{app}. In the Parkinson's disease and healthy aged control groups, the magnitude of K^{app} was significantly decreased in the medial frontal cortex, whereas the magnitude of K was greater in medial frontal cortex of both the aged control and Parkinson's disease groups, relative to the young control subjects. The magnitudes of K_{in}^{app} and K^{app} were reduced in the putamen but not caudate nucleus of the Parkinson's disease group relative to the both

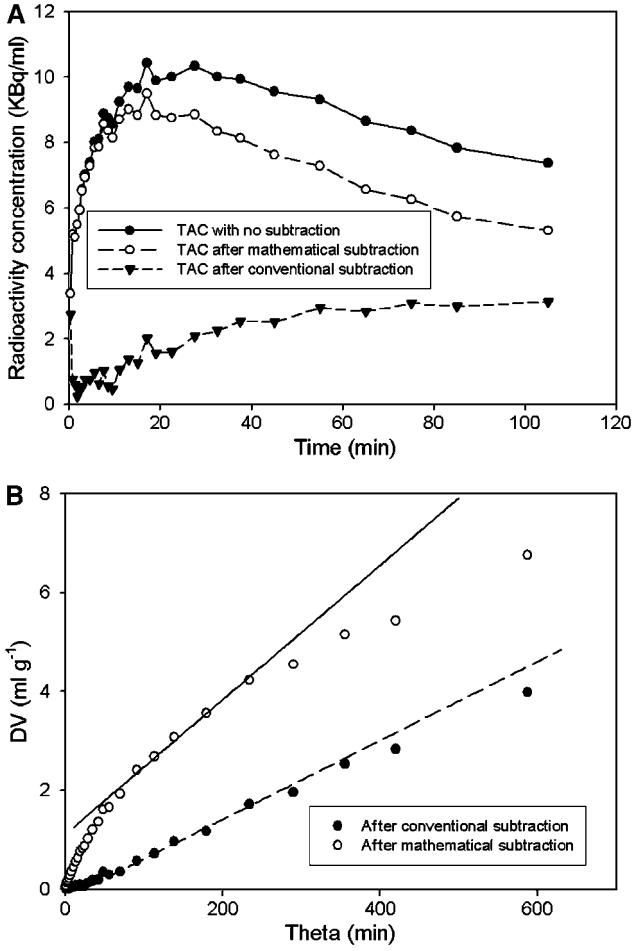

Figure 3 Effect of subtraction of the calculated 3-*O*-methyl-[^{18}F]FDOPA (OMFD) concentration in the brain on the estimation of net FDOPA influx. (**A**) The measured time–radioactivity curve in the putamen of a patient with Parkinson's disease, along with the corresponding curve calculated by subtraction of the estimated brain OMFD curve, and (**B**) Plots of the distribution volumes (DV) corresponding to the same data by the methods of K_{in}^{app} (●) and K^{app} (○) as functions of the normalized arterial [^{18}F]fluorodopa (FDOPA) input. Regression lines are calculated for data recorded during the interval 20 to 60 mins.

Table 2 The population mean rate constants for the relative activity of catechol-*O*-methyltransferase with respect to FDOPA in plasma (k_0^D, min^{-1}) and for the elimination rate constant of OMFD from plasma (k_{-1}^M, min^{-1})

	Normal <50 years (n = 7)	*Normal >50 years* (n = 8)	*Parkinson's disease* (n = 5)
k_0^D	0.0127 ± 0.0030	0.0128 ± 0.0037	0.0106 ± 0.0012
k_{-1}^M	0.0212 ± 0.0051	0.0097 ± 0.0051*	0.00598 ± 0.0005*

*Significantly different than estimate obtained in the young normal group. $P < 0.001$.

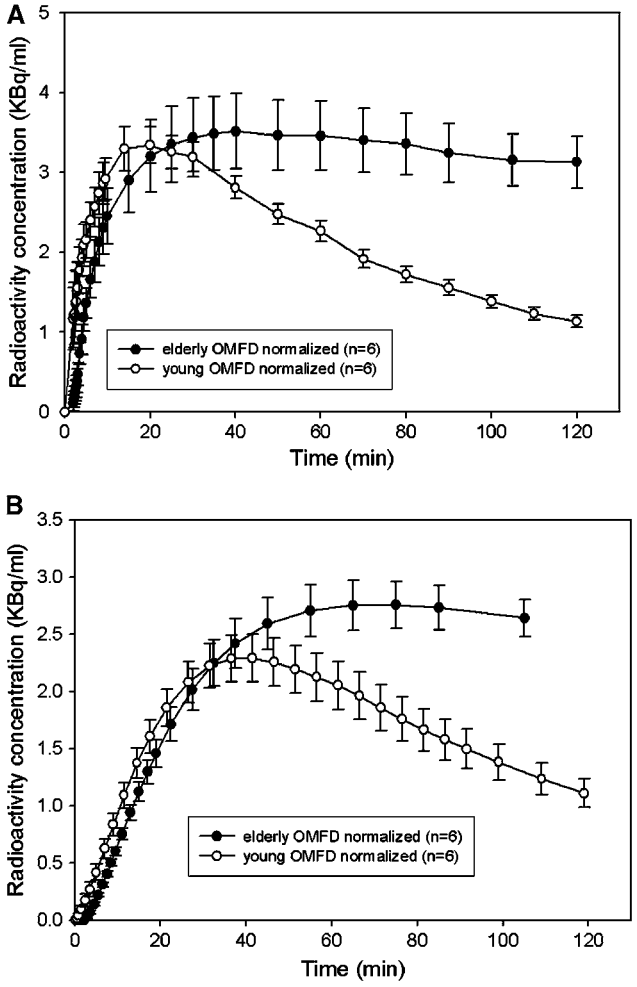

Figure 4 Mean concentrations of 3-*O*-methyl-[^{18}F]FDOPA (OMFD) measured in plasma and normalized to a common [^{18}F]fluorodopa (FDOPA) input (**A**), and the normalized concentrations calculated in the cerebellum using a constrained compartmental model (**B**) in healthy young subjects (26.0 ± 3.5 years) and healthy elderly subjects (61.0 ± 7.1 years). Each estimate is the mean $\pm$ s.e.m. of six determinations. At times after 50 mins, the normalized plasma and brain OMFD radioactivities of these two populations were significantly different (unpaired *t*-test, $P < 0.05$).

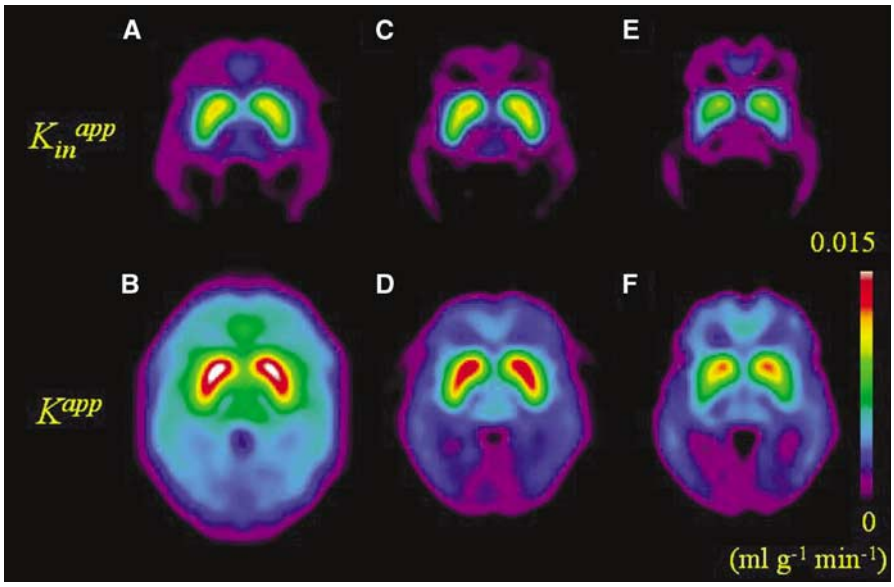

Figure 5 Parametric maps of the net influx of [^{18}F]fluorodopa (FDOPA) to the brain calculated by the subtraction of the cerebellum time–radioactivity curve (TAC) (K_{in}^{app}; upper row) and after subtraction of the calculated brain TAC for 3-*O*-methyl-[^{18}F]FDOPA (OMFD) (K^{app}; lower row). Images are the mean of the maps obtained in healthy normal subjects under the age of 50 years (**A**, **B**; $n=7$; 27.6 ± 5.2 years old), in healthy older subjects (**C**, **D**; $n=8$; 59.0 ± 7.1 years old) and in patients with Parkinson's disease (**E**, **F**; $n=5$; 62.0 ± 8.2 years old). Average images were obtained by spatial normalization of the individual influx maps to the MNI stereotaxic brain and by blurring with a Gaussian kernel of 12 mm full-width at half-maximum.

Table 3 Summary of the net blood–brain clearance of FDOPA calculated by the conventional method with subtraction of the total cerebellum radioactivity (K_{in}^{app}, mL/g min), and after subtraction of the calculated brain OMFD with (K^{app}, mL/g min), using data recorded in the interval of 20 to 60 mins in the medial frontal cortex, caudate, and putamen

	Normal <50 years (n = 7)	*Normal >50 years* (n = 8)	*Parkinson's disease* (n = 5)
Medial frontal cortex			
K_{in}^{app}	0.0007 ± 0.0008	-0.0002 ± 0.0012	-0.0004 ± 0.0010
K^{app}	0.0049 ± 0.0012	0.0026 ± 0.0019*	$0.0024\pm0.0010^{\$\$}$
K	0.0061 ± 0.0016	0.0121 ± 0.0059*	$0.0181\pm0.0074^{\$\$}$
k_{loss}	0.0036 ± 0.0013	0.023 ± 0.014**	$0.032\pm0.010^{\$\$\$}$
EDV^2	1.98 ± 0.89	0.66 ± 0.34**	$0.56\pm0.13^{\$\$}$
Caudate			
K_{in}^{app}	0.0082 ± 0.0021	0.0081 ± 0.0017	0.0071 ± 0.0031
K^{app}	0.0125 ± 0.0034	0.0108 ± 0.0024	0.0099 ± 0.0034
K	0.0135 ± 0.0038	0.0132 ± 0.0025	0.0142 ± 0.0037
k_{loss}	0.0013 ± 0.0008	0.0035 ± 0.0017**	$0.0064\pm0.0015^{\$\$\$,\#}$
EDV^2	13.8 ± 7.2	4.8 ± 2.8**	$2.4\pm1.2^{\$\$,\#}$
Putamen			
K_{in}^{app}	0.0124 ± 0.0023	0.0135 ± 0.0018	$0.0086\pm0.0010^{\$\$,\#\#}$
K^{app}	0.0166 ± 0.0035	0.0162 ± 0.0017	$0.0114\pm0.0018^{\$,\#\#}$
K	0.0180 ± 0.0034	0.0196 ± 0.0024	0.0200 ± 0.0027
k_{loss}	0.00164 ± 0.0008	0.0037 ± 0.0015**	$0.0094\pm0.0020^{\$\$\$,\#\#}$
EDV^2	14.2 ± 7.7	6.0 ± 2.6*	$2.2\pm0.5^{\$\$,\#\#}$

Also presented are the results of nonlinear fittings after subtraction of the calculated brain OMFD for the estimation of net clearance (K, mL/g min) corrected for diffusion of [^{18}F]fluorodopamine and its metabolites from brain (k_{loss}, min^{-1}), using data recorded in the interval 10 to 120 mins. The effective distribution volume for FDOPA (EDV^2, mL/g) was calculated as the ratio K/k_{loss}.

Significant difference between normal <50 years old and normal >50 years old: *$P<0.05$, **$P<0.01$. Significant difference between Parkinson's disease group and normal <50 years: $^{\$}P<0.05$, $^{\$\$}P<0.01$, $^{\$\$\$}P<0.0001$. Significant difference between Parkinson's disease group and normal >50 years old: $^{\#}P<0.05$, $^{\#\#}P<0.01$. Differences between estimates of K_{in}^{app} and K^{app} were significant in the frontal cortex ($P<0.05$) and in the caudate and putamen ($P<0.01$). Differences between estimates of K_{in}^{app} and K were significant ($P<0.005$) in all regions and groups.

normal control groups. There were no significant differences between the magnitudes of K_{in}^{app}, K^{app} or K in the caudate or putamen of the healthy aged and young groups. The magnitude of k_{loss} in the medial frontal cortex, caudate and putamen was significantly increased in healthy aged controls as compared with

young control subjects, and was also increased in patients with Parkinson's disease in comparison to both the young and aged healthy control groups (Table 3). Conversely, the magnitude of the ratio EDV^2 was significantly reduced in the frontal cortex, caudate, and putamen of healthy aged controls as compared with young control subjects, and was further reduced in caudate and putamen of patients with Parkinson's disease in comparison to healthy young and aged control subjects (Table 3).

Discussion

The presence of substantial amounts of the brain-penetrating metabolite OMFD in plasma remains a major issue in the quantitation of PET studies with FDOPA (Sossi *et al*, 2003). In the original description of K_{in}^{app}, it was assumed that the OMFD concentrations in the reference region and striatum are identical (Martin *et al*, 1989), a claim that has been supported by PET investigations of the brain distribution of OMFD (Wahl *et al*, 1994; Dhawan *et al*, 1996). Thus, subtraction of the total radioactivity in the reference region is an appropriate correction for the OMFD radioactivity in the VOI, assuming that brain COMT activity does not heterogeneously alter the relationship between brain FDOPA and OMFD concentrations (Cumming and Gjedde, 1998). However, it does not follow that subtraction of the total reference tissue radioactivity correctly isolates the summed brain radioactivities of FDOPA and its decarboxylated metabolites.

Based on the definition of net blood–brain clearance, the total distribution volume of FDOPA together with its decarboxylated metabolites in an VOI must be underestimated after subtraction of the total radioactivity concentration in the nonbinding reference region, even if the FDOPA concentrations in the two brain regions were identical. However, the precursor pool in striatum of rat (Cumming *et al*, 1987*a*) and monkey (Endres *et al*, 2004) is progressively depleted relative to the cerebellum because of high activity of DOPA decarboxylase in the former tissue. Thus, subtraction of the reference tissue total radioactivity produces in some brain regions an *oversubtraction* of the precursor pool for [^{18}F]fluorodopamine synthesis. This phenomenon underlies the offset of some 15 mins after FDOPA injection before the calculation of positive [^{18}F]fluorodopamine concentrations in human putamen (present Figure 3A, and see Martin *et al*, 1989), even though biochemical studies *ex vivo* show that high concentrations of [^{18}F]fluorodopamine are present in rat striatum within minutes of FDOPA injection (Cumming *et al*, 1988, 1993).

For the above reasons, the conventional calculation of K_{in}^{app} is *a priori* expected to underestimate the true magnitude of the net influx of FDOPA to brain regions containing the enzyme DOPA decarboxylase. In the present study, we have attempted to make a more correct subtraction of the brain radioactivity attributable to OMFD entering from circulation, calculated using a constrained compartmental model; this subtraction makes evident the presence of FDOPA and its decarboxylated metabolites in the putamen in the early phase of the PET recording (Figure 3A). As predicted from the above discussion, we find the magnitude of K^{app} to be positively offset with respect to the corresponding estimates of K_{in}^{app} (Figure 3B). The magnitude of this offset or bias, evident to visual inspection of the influx maps (Figure 5) was uniformly 0.0042 mL/g min in the brain of the healthy young subjects and 0.0027 mL/g min in the healthy elderly and Parkinson's disease subjects (Table 2). In relative terms, the bias of K_{in}^{app} was particularly great in the cerebral cortex, where the magnitude of K_{in}^{app} is normally close to zero. Insofar as the net blood–brain clearance of FDOPA is an index of levodopa utilization, the present analysis suggests that cortical levodopa utilization may have been substantially underestimated in previous FDOPA/PET studies using linear graphical analysis. Indeed, results presented in Table 3 suggest that the intrinsic FDOPA consumption in cerebral cortex may have been underestimated by a factor of 10 in previous analyses.

In principal, bias in the estimation of K_{in}^{app} because of the oversubtraction of the precursor pool in the brain might properly be assessed in PET studies in which the activity of peripheral COMT was pharmacologically blocked. Indeed, pharmacological blockade of COMT greatly enhances the formation of [^{18}F]fluorodopamine in striatum of rats (Cumming *et al*, 1987*b*) and monkey (Günther *et al*, 1995). However, blockade of COMT with entacapone did not substantially alter the magnitude of the striatal activity of DOPA decarboxylase (k_3^D, min^{-1}) in patients with Parkinson's disease (Ruottinen *et al*, 1997). Relative to a drug-free baseline condition, the peripherally acting COMT inhibitor entacapone (OR-611) decreased the net FDOPA influx calculated relative to an occipital cortex input in Parkinson's disease patients, but not in healthy control subjects (Ruottinen *et al*, 1995), whereas a centrally acting COMT inhibitor (tolcapone) was without effect on the magnitude of K_{in}^{app} in monkey striatum (Doudet *et al*, 1997). Treatment with entacapone was without effect on the estimation of K_{in}^{app} in human patients with Parkinson's disease (Ishikawa *et al*, 1996*b*), but decreased the magnitude of K_{in}^{app} in healthy monkey striatum (Léger *et al*, 1998); in both studies COMT inhibition revealed the sensitivity of the compartmental modeling approach to the presence in plasma of OMFD. Together, the results of these studies suggest that effects of OMFD on the estimation of FDOPA net influx cannot be unambiguously assessed by pharmacological blockade of COMT because of the confounding effects of pharmacological treatment on blood–brain transport and central metabolism.

In the present study, we have replicated our earlier finding that, whereas the relative activity of whole body COMT with respect to FDOPA in plasma (k_0^D) was nearly identical in the present three groups, the rate constant for elimination of OMFD from plasma (k_{-1}^D) was reduced in the elderly, a phenomenon, which may be related to impaired renal clearance (Cumming *et al*, 1993). Consequently, after normalization to a common AUC for the arterial FDOPA input, we find that the AUCs for OMFD were significantly increased by 44% in plasma (Figure 4A). After normalization, the cerebellum concentrations of OMFD were greater in the healthy elderly subjects at times after 50 mins, although the final AUCs did not differ (Figure 4B). Thus, after normalization the temporal changes in the ratio between FDOPA (not shown) and OMFD concentrations in the reference region may be distinct in the young and old. This phenomenon may have consequences for the estimation of FDOPA utilization using reference tissue methods (Hoshi *et al*, 1993).

Previous studies have revealed k_3^s, a reference-tissue index of FDOPA utilization, to be unchanged in frontal cortex of patients with bilateral Parkinson's disease, but increased in hemi-Parkinson's disease (Rakshi *et al*, 1999), whereas others find K_{in}^{app} to be increased in frontal cortex of Parkinson's disease (Kaasinen *et al*, 2001). While the present maps of K^{app} do not suggest a difference in FDOPA utilization in frontal cortex of the present group of five Parkinson's disease patients relative to the healthy elderly, they do reveal a hitherto unreported decline of FDOPA utilization throughout the neocortex in the healthy aged group (see Table 3), which is less evident to inspection of the corresponding K_{in}^{app} maps (Figure 5). This difference in K^{app} was statistically significant in the VOI analysis, suggesting that cortical FDOPA utilization indeed declines with normal ageing. Nonetheless, the magnitude of the estimate of K was greater in medial frontal cortex of both elderly subject groups than in the healthy young subjects. However, this parameter may tend to be overestimated in brain regions with low intrinsic FDOPA utilization and relatively poor storage, because of the trade-off between the estimations K and k_{loss} when the specific signal is low.

In the present approach, the [^{18}F]fluorodopamine and its subsequent metabolites ([^{18}F]fluoro-DOPAC and [^{18}F]fluoro-HVA) are assumed to diffuse from the brain as a single metabolic compartment. Separate rate constants for the catabolism of [^{18}F]fluorodopamine by monoamine oxidase (k_7) and for the diffusion of its acidic metabolites from the brain (k_9) have been calculated on the basis of biochemical studies *ex vivo* (Cumming *et al*, 1994), and have been arbitrarily fixed as equal in an earlier FDOPA/PET analysis (Kuwabara *et al*, 1993). While these two parameters cannot be distinguished in the present graphical analysis, their composite determines the magnitude of k_{loss}. We have earlier argued that the activity of monoamine oxidase with respect to labeled dopamine is a function of the partitioning of substrate between the cytosolic and vesicular compartments (Deep *et al*, 1997). As such, the magnitude of k_{loss} is a surrogate marker for the vesicular storage capacity. The present finding of relatively high k_{loss} in the cerebral cortex is consistent with earlier biochemical findings in rat hippocampus (Cumming *et al*, 1995), suggesting that the [^{18}F]fluorodopamine formed in extrastriatal regions may be particularly unprotected from catabolism by monoamine oxidase. However, we have argued above that the simultaneous determinations of K and k_{loss} may be unreliable in the cerebral cortex because of the low specific signal in that tissue.

Using the K_{in} method, we have earlier estimated the magnitude of k_{loss} to be 0.004 min^{-1} in the striatum of living pigs with 120-min-long FDOPA emission recordings, although the variability of the estimate of k_{loss} was very high (Danielsen *et al*, 1999). In the present study, we were unable to obtain stable estimates of K_{in} and k_{loss} in human FDOPA recordings of 120-min duration, but were able to estimate K and k_{loss}. However, the magnitude of K in striatum did not differ between normal young, normal aged, and Parkinson's disease patients in the present study. We have earlier shown that the simultaneous determination of K and k_4 in the case of FDG is dependent on the duration of the recording (Kuwabara *et al*, 1990; Kuwabara and Gjedde, 1991) because of the interrelationship of the kinetically estimated rate constants k_2, k_3 and k_4 (or k_{loss}) from imperfect data. In the present context, the inherent value of K is, by definition, the unknowable slope of the net FDOPA uptake plot at time zero before any washout has taken place. Thus, in the present study, uncertainty in the estimation of K is compounded in the striatum of the elderly and Parkinson's disease subjects, in whom the capacity for [^{18}F]fluorodopamine storage is apparently impaired. This phenomenon may contribute to the lack of disease-sensitivity of K in the present study.

As shown in Figure 3B, curvature of the conventional K_{in}^{app} plots in the striatum is discernible after only 60 mins of FDOPA circulation, but this curvature was inadequate for the stable estimation of K_{in} and k_{loss} with 120-min recordings. In contrast, early curvature is clearly evident in the K^{app} plots, facilitating the estimation of k_{loss} using the nonlinear method for calculating K. The magnitude of the present estimate of k_{loss} in the caudate and putamen of healthy young adults (0.0015 min^{-1}) was close to earlier estimates obtained by the K_{in} analysis of 240-min-long recordings from healthy non-human primates (Cumming *et al*, 2001) and human control subjects (Sossi *et al*, 2002), also with 240-min-long recordings. We conclude that the present mathematical subtraction of the brain OMFD unmasks the curvature in the influx plots already present within 120 mins. This finding presents a clear advantage for the design of FDOPA studies, since the 240-min-long

recordings are poorly tolerated by healthy volunteers and Parkinson's disease patients.

The apparently superior sensitivity of the present kinetic metabolite subtraction method for estimating k_{loss} could be related to the progressive disappearance of FDOPA from plasma and the cerebellum, such that there is a considerable delay before the over-subtraction of the brain FDOPA becomes insignificant for the calculation of K_{in}, that is, when the concentration of FDOPA approaches zero in all brain regions. Relative to the young group, we find that the magnitude of k_{loss} in the striatum of the healthy elderly was two-fold elevated, whereas the EDV^2 was two-fold reduced, suggesting an age-related impairment of the capacity to store [^{18}F]fluorodopamine in synaptic vesicles. Comparison with the results obtained in the Parkinson's disease group suggests that the neurologic disease is associated with a further two-fold increase in k_{loss} and two-fold decrease in EDV^2 in excess of the decline related to normal ageing, in close agreement with a recent comparison of EDV^1 in healthy age-matched control subjects and patients with early Parkinson's disease (Sossi *et al*, 2004).

Consistent with the present results, the magnitude of k_{loss} has been found to be elevated two–three-fold in the striatum of monkeys with MPTP-induced parkinsonism (Doudet *et al*, 1997; Sossi *et al*, 2001; Cumming *et al*, 2001), and in patients with idiopathic Parkinson's disease (Sossi *et al*, 2002). The present estimates of the magnitude of k_{loss} predict that the half-life for [^{18}F]fluorodopamine formed in the caudate and putamen declines from 7 h in the healthy young to 3 h in the healthy elderly, and only 75 mins in patients with early Parkinson's disease (Hoehn and Yahr II). The latter calculation of impaired retention of newly synthesized dopamine seems consistent with the duration of clinical response to levodopa treatment in early Parkinson's disease (Cumming *et al*, 1999).

In the present study, the magnitudes of K_{in}^{app} (and K^{app}) were significantly reduced by one third in the putamen (but not the caudate nucleus) of the Parkinson's disease patients relative to the healthy aged controls and the young control subjects. This finding of reduced FDOPA net influx specifically to the putamen of Parkinson's disease patients is consistent with a large number of previous PET studies (Snow *et al*, 1990; Bhatt *et al*, 1991; Hoshi *et al*, 1993; Ishikawa *et al*, 1996*a*; Vingerhoets *et al*, 1996; de la Fuente-Fernández *et al*, 2000; Rousset *et al*, 2000). The magnitudes of K_{in}^{app} and K^{app} (and K) in the striatum were not significantly different between the present groups of healthy young and aged subjects, in agreement with a large number of earlier PET studies failing to detect age-related alterations in FDOPA utilization in the striatum in the absence of neurologic disease (see Cumming and Gjedde, 1998). However, the apparent stability of striatal FDOPA utilization with normal aging seems surprising; *post mortem* histologic (McGeer *et al*, 1977) and immunohistochemical studies (Cabello *et al*, 2002) have earlier shown loss of pigmented neurons in the substantia nigra at a rate of approximately 7% per decade of healthy aging. Furthermore, the specific binding of the vesicular transporter ligand [^{11}C]dihydrotetrabenazine in living striatum of healthy humans declines by 6% per decade (Taylor *et al*, 2000), which predicts a decline in the capacity for [^{18}F]fluorodopamine retention in the aged brain. Thus, the present finding of reduced EDV^2 with healthy ageing is consistent with some earlier reports of a progressive impairment of other markers of the integrity of dopamine neurons, but constitutes the first report of changes in striatal FDOPA metabolism and trapping as a function of normal aging. Furthermore, the present analyses of k_{loss} and EDV^2 have detected changes in the caudate nucleus of Parkinson's disease patients, which were not evident in the linear graphical analyses of that structure.

We have earlier reported regulation of the activity of DOPA decarboxylase in living rat striatum (Cumming *et al*, 1995). Previous PET studies suggest FDOPA influx is less impaired than is [^{11}C]dihydrotetrabenazine binding in striatum of patients with early Parkinson's disease, suggesting that increases in FDOPA utilization can occur in compensation for reduced [^{18}F]fluorodopamine storage capacity (Lee *et al*, 2000). This phenomenon has been invoked to explain the greater sensitivity of EDV^1 than K_{in}^{app} in the discrimination of normal and Parkinson's disease patients (Sossi *et al*, 2004). Indeed, all the net influx terms defined in Table 2 might be perturbed by compensatory mechanisms so as to optimize FDOPA utilization in patients with an early stage of Parkinson's disease. On the basis of the present findings, we furthermore suggest that compensatory increases in the utilization of FDOPA can accommodate a premorbid decline in [^{18}F]fluorodopamine storage capacity occurring with normal ageing. As such, the kinetic parameter k_{loss} may more aptly reveal nonpathological declines and disease-related decompensation of FDOPA utilization than do the net influx parameters, which are relatively insensitive indices of age- and disease-related changes (Table 3).

In summary, we have developed a new approach for quantitative analysis of FDOPA influx to the brain. Using a constrained compartmental analysis, we first estimated the brain concentration of the plasma metabolite OMFD, and then subtracted this concentration frame-by-frame from all voxels, before calculation of the net influx by linear regression (K^{app}). Consistent with theory, we find that over-subtraction of the precursor pool in the conventional linear analysis of FDOPA influx (K_{in}^{app}) results in a global negative bias relative to K^{app}. The present method reveals an age-related decline in the magnitude of FDOPA utilization in the medial frontal cortex, apparently obscured by the presence of brain OMFD. The new method furthermore reveals the

early curvature of influx plots, such that the magnitude of k_{loss} and the EDV[2] can be estimated from 120-min-long emission recordings. This analysis reveals for the first time an age-related decline in the storage capacity for [^{18}F]fluorodopamine formed in normal human striatum, and supports earlier findings that storage capacity is a more sensitive marker of the integrity of dopamine innervations than are estimates of the net FDOPA influx to brain.

References

Bhatt MH, Snow BJ, Martin WR, Pate BD, Ruth TJ, Calne DB (1991) Positron emission tomography suggests that the rate of progression of idiopathic parkinsonism is slow. *Ann Neurol* 29:673–7

Bonuccelli U, Piccini P, Del Dotto P, Rossi G, Corsini GU, Muratorio A (1993) Apomorphine test for dopaminergic responsiveness: a dose assessment study. *Mov Disord* 8:158–64

Boyes BE, Cumming P, Martin WR, McGeer EG (1986) Determination of plasma [^{18}F]-6-fluorodopa during positron emission tomography: elimination and metabolism in carbidopa treated subjects. *Life Sci* 39: 2243–2252

Cabello CR, Thune JJ, Pakkenberg H, Pakkenberg B (2002) Ageing of substantia nigra in humans: cell loss may be compensated by hypertrophy. *Neuropathol Appl Neurobiol* 28:282–91

Collins DL, Zijdenbos AP, Kollokian V, Sled JG, Kabani NJ, Holmes CJ, Evans AC (1998) Design and construction of a realistic digital brain phantom. *IEEE Trans Med Imaging* 17:463–8

Cumming P, Boyes BE, Martin WRW, Adam M, Grierson J, Ruth T, McGeer EG (1987*a*) The metabolism of [^{18}F]fluoro-L-3,4-dihydroxyphenylalanine in the hooded rat. *J Neurochem* 48:601–8

Cumming P, Boyes BE, Martin WRW, Adam M, Ruth TJ, McGeer EG (1987*b*) Altered metabolism of [^{18}F]-6-fluorodopa in the hooded rat following inhibition of catechol-*O*-methyltransferase with U-0521. *Biochem Pharmacol* 36:2527–31

Cumming P, Hausser M, Martin WR, Grierson J, Adam MJ, Ruth TJ, McGeer EG (1988) Kinetics of *in vitro* decarboxylation and the *in vivo* metabolism of 2-^{18}F- and 6-^{18}F-fluorodopa in the hooded rat. *Biochem Pharmacol* 37:247–50

Cumming P, Léger GC, Kuwabara H, Gjedde A (1993) Pharmacokinetics of plasma 6-[^{18}F]fluoro-L-3,4-dihydroxyphenylalanine ([^{18}F]Fdopa) in humans. *J Cereb Blood Flow Metab* 13:668–75

Cumming P, Kuwabara H, Gjedde A (1994) A kinetic analysis of [^{18}F]-6-fluoro-L-dihydroxyphenylalanine ([^{18}F]DOPA) metabolism in the rat. *J Neurochem* 63:1675–82

Cumming P, Kuwabara H, Ase A, Gjedde A (1995) Regulation of DOPA decarboxylase activity in brain of living rat. *J Neurochem* 65:1381–90

Cumming P, Gjedde A, Reith J (1997) Controversies arising from recent FDOPA articles [Letter]. *J Nucl Med* 38:1267–9

Cumming P, Hermansen F, Gjedde A (1999) Cerebral dopamine concentrations during levodopa treatment [Letter]. *Neurology* 53:1374

Cumming P, Gjedde A (1998) Compartmental analysis of dopa decarboxylation in living brain from dynamic positron emission tomograms. *Synapse* 29:37–61

Cumming P, Munk OL, Doudet D (2001) Loss of metabolites from monkey striatum during PET with FDOPA. *Synapse* 41:212–8

Danielsen EH, Smith DF, Venkatachalam TK, Hansen SB, Gjedde A, Cumming P (1999) Cerebral ^{18}F-DOPA metabolism in the immature pig brain studied by positron emission tomography. *Synapse* 33:247–58

Deep P, Gjedde A, Cumming P (1997) On the accuracy of an [^{18}F]FDOPA compartmental model: evidence for vesicular storage of 6-[^{18}F]fluorodopamine *in vivo*. *J Neurosci Met* 76:157–65

Dhawan V, Ishikawa T, Patlak C, Chaly T, Robeson W, Belakhef A, Margouleff C, Mandel F, Eidelberg D (1996) Combined FDOPA and 3OMFD PET studies in Parkinson's disease. *J Nucl Med* 37:209–16

Dhawan V, Ishikawa T, Patlak C, Eidelberg D (1997) Controversies arising from recent FDOPA articles [Letter]. *J Nucl Med* 38:1270–1

de la Fuente-Fernández R, Pal PK, Vingerhoets FJ, Kishore A, Schulzer M, Mak EK, Ruth TJ, Snow BJ, Calne DB, Stoessl AJ (2000) Evidence for impaired presynaptic dopamine function in parkinsonian patients with motor fluctuations. *J Neural Transm* 107:49–57

Doudet DJ, Chan GL, Holden JE, Morrison KS, Wyatt RJ, Ruth TJ (1997) Effects of catechol-*O*-methyltransferase inhibition on the rates of uptake and reversibility of 6-fluoro-L-Dopa trapping in MPTP-induced parkinsonism in monkeys. *Neuropharmacology* 36:363–71

Doudet DJ, Chan GL, Holden JE, McGeer EG, Aigner TA, Wyatt RJ, Ruth TJ (1998) 6-[^{18}F]Fluoro-L-DOPA PET studies of the turnover of dopamine in MPTP-induced parkinsonism in monkeys. *Synapse* 29:225–32

Endres CJ, DeJesus OT, Uno H, Doudet DJ, Nickles RJ, Holden JE (2004) Time profile of cerebral [^{18}F]6-fluoro-L-dopa metabolites in non-human primate: Implications for the kinetics of therapeutic L-DOPA. *Frontiers Biosci* 9:505–12

Garnett ES, Firnau G, Nahmias C (1983) Dopamine visualized in the basal ganglia of living man. *Nature* 305:137–8

Gillings NM, Bender D, Falborg L, Marthi K, Munk OL, Cumming P (2001) Kinetics of the metabolism of four PET radioligands in living minipigs. *Nucl Med Biol* 28:97–104

Gjedde A (1981) High- and low-affinity transport of D-glucose from blood to brain. *J Neurochem* 36: 1463–1471

Gjedde A (1982) Calculation of cerebral glucose phosphorylation from brain uptake of glucose analogs *in vivo*: a re-examination. *Brain Res* 257:237–74

Gjedde A (1988) Exchange diffusion of large neutral amino acids between blood and brain. In: *Peptide and amino acid transport mechanisms in the central nervous system* (Rakic L *et al*, eds) New York: Stockton Press, 209–17

Gjedde A, Reith J, Dyve S, Léger G, Guttman M, Diksic M, Evans A, Kuwabara H (1991) Dopa decarboxylase activity of the living human brain. *Proc Natl Acad Sci USA* 88:2721–5

Gjedde A, Léger GC, Cumming P, Yasuhara Y, Evans AC, Guttman M, Kuwabara H (1993) Striatal L-dopa decarboxylase activity in Parkinson's disease *in vivo*: implications for the regulation of dopamine synthesis. *J Neurochem* 61:1538–41

Günther I, Psylla M, Reddy GN, Antonini A, Vontobel P, Reist HW, Zollinger A, Nickles RJ, Beer HF, Schubiger PA, Leenders KL (1995) Positron emission tomography in drug evaluation: influence of three different catechol-*O*-methyltransferase inhibitors on metabolism of 6-[^{18}F]fluoro-L-dopa in rhesus monkey. *Nucl Med Biol* 22:921–7

Holden JE, Doudet D, Endres CJ, Chan GL-Y, Morrison KS, Vingerhoets FJG, Snow BJ, Pate BD, Sossi V, Buckley KR, Ruth TJ (1997) Graphical analysis of 6-fluoro-L-dopa trapping: Effect of inhibition of catechol-*O*-methyltransferase. *J Nucl Med* 38:1568–74

Horne MK, Cheng CH, Wooten GF (1984) The cerebral metabolism of L-dihydroxyphenylalanine: an autoradiographic and biochemical study. *Pharmacology* 28:12–26

Hoshi H, Kuwabara H, Léger G, Cumming P, Guttman M, Gjedde A (1993) 6-[^{18}F]fluoro-L-dopa metabolism in living human brain: a comparison of six analytical methods. *J Cereb Blood Flow Metab* 13:57–69

Huang SC, Yu DC, Barrio JR, Grafton S, Melega WP, Hoffman JM, Satyamurthy N, Mazziotta JC, Phelps ME (1991) Kinetics and modeling of L-6-[^{18}F]fluoro-dopa in human positron emission tomographic studies. *J Cereb Blood Flow Metab* 11:898–913

Ishikawa T, Dhawan V, Chaly T, Margouleff C, Robeson W, Dahl JR, Mandel F, Spetsieris P, Eidelberg D (1996*a*) Clinical significance of striatal DOPA decarboxylase activity in Parkinson's disease. *J Nucl Med* 37:216–22

Ishikawa T, Dhawan V, Chaly T, Robeson W, Belakhlef A, Mandel F, Dahl R, Margouleff C, Eidelberg D (1996*b*) Fluorodopa positron emission tomography with an inhibitor of catechol-*O*-methyltransferase: effect of the plasma 3-*O*-methyldopa fraction on data analysis. *J Cereb Blood Flow Metab* 16:854–63

Kaasinen V, Nurmi E, Brück A, Eskola O, Bergman J, Solin O, Rinne JO (2001) Increased frontal [^{18}F]fluorodopa uptake in early Parkinson's disease: sex differences in the prefrontal cortex. *Brain* 124:1125–30

Kumakura Y, Danielsen EH, Reilhac A, Gjedde A, Cumming P (2004) The influx of [^{18}F]fluorodopa to brain of normal volunteers and patients with Parkinson's disease: effect of levodopa. *Acta Neurol Scand* 110:188–95

Kuwabara H, Evans AC, Gjedde A (1990) Michaelis–Menten constraints improved cerebral glucose metabolism and regional lumped constant measurements with [^{18}F]fluorodeoxyglucose. *J Cereb Blood Flow Metabol* 10:180–9

Kuwabara H, Gjedde A (1991) Measurements of glucose phosphorylation with FGD phosphate and PET are not reduced by dephosphorylation of FDG-6-phosphate. *J Nucl Med* 32:692–8

Kuwabara H, Cumming P, Reith J, Léger G, Diksic M, Evans A, Gjedde A (1993) Human striatal L-DOPA decarboxylase activity estimated *in vivo* using 6-[^{18}F]fluoro-DOPA and positron emission tomography: Error analysis and applications to normal subjects. *J Cereb Blood Flow Metab* 13:43–56

Lee CS, Samii A, Sossi V, Ruth TJ, Schulzer M, Holden JE, Wudel J, Pal PK, de la Fuente-Fernández R, Calne DB, Stoessl AJ (2000) *In vivo* positron emission tomographic evidence for compensatory changes in presynaptic dopaminergic nerve terminals in Parkinson's disease. *Ann Neurol* 47:493–503

Léger G, Gjedde A, Kuwabara H, Guttman M, Cumming P (1998) Effect of catechol-O-methyltransferase inhibition on brain uptake of [^{18}F]fluorodopa: implications for compartmental modelling and clinical usefulness. *Synapse* 30:351–61

Martin WR, Palmer MR, Patlak CS, Calne DB (1989) Nigrostriatal function in humans studied with positron emission tomography. *Ann Neurol* 26:535–42

McGeer PL, McGeer EG, Suzuki JS (1977) Aging and extrapyramidal function. *Arch Neurol* 34:33–5

Melega WP, Grafton ST, Huang SC, Satyamurthy N, Phelps ME, Barrio JR (1991) L-6-[^{18}F]fluorodopa metabolism in monkeys and humans: biochemical parameters for the formulation of tracer kinetic models with positron emission tomography. *J Cereb Blood Flow Metab* 11:890–7

Patlak CS, Blasberg RG, Fenstermacher JD (1983) Graphical evaluation of blood-to-brain transfer constants from multiple-time uptake data. *J Cereb Blood Flow Metab* 3:1–7

Patlak CS, Blasberg RG (1985) Graphical evaluation of blood-to-brain transfer constants from multiple-time uptake data. *Generalizations. J Cereb Blood Flow Metab* 5:584–90

Psylla M, Gunther I, Antonini A, Vontobel P, Reist HW, Zollinger A, Leenders KL (1997) Cerebral 6-[^{18}F]fluoro-L-DOPA uptake in rhesus monkey: pharmacological influence of aromatic amino acid decarboxylase (AAAD) and catechol-*O*-methyltransferase (COMT) inhibition. *Brain Res* 767:45–54

Rakshi JS, Uema T, Ito K, Bailey DL, Morrish PK, Ashburner J, Dagher A, Jenkins IH, Friston KJ, Brooks DJ (1999) Frontal, midbrain and striatal dopaminergic function in early and advanced Parkinson's disease A 3D [^{18}F]dopa-PET study. *Brain* 122:1637–50

Reilhac A, Sechet S, Boileau I, Gunn R, Evans A, Dagher A (2003) Motion correction for PET ligand imaging. *NeuroImage* **19**; Part 2 of 2 parts, S46 (poster #927). PROGRAM. *Human Brain Mapping 2003*, New York, June 18–22, 2003.

Rousset OG, Deep P, Kuwabara H, Evans AC, Gjedde AH, Cumming P (2000) Effect of partial volume correction on estimates of the influx and cerebral metabolism of 6-[^{18}F]fluoro-L-dopa studied with PET in normal control and Parkinson's disease subjects. *Synapse* 37:81–9

Ruottinen HM, Rinne JO, Ruotsalainen UH, Bergman JR, Oikonen VJ, Haaparanta MT, Solin OH, Laihinen AO, Rinne UK (1995) Striatal [^{18}F]fluorodopa utilization after COMT inhibition with entacapone studied with PET in advanced Parkinson's disease. *J Neural Transm Park Dis Dement Sect* 10:91–106

Ruottinen HM, Rinne JO, Oikonen VJ, Bergman JR, Haaparanta MT, Solin OH, Ruotsalainen UH, Rinne UK (1997) Striatal 6-[^{18}F]fluorodopa accumulation after combined inhibition of peripheral catechol-*O*-methyltransferase and monoamine oxidase type B: differing response in relation to presynaptic dopaminergic dysfunction. *Synapse* 27:336–46

Snow BJ, Peppard RF, Guttman M, Okada J, Martin WR, Steele J, Eisen A, Carr G, Schoenberg B, Calne D (1990) Positron emission tomographic scanning demonstrates a presynaptic dopaminergic lesion in Lytico-Bodig. The amyotrophic lateral sclerosis-parkinsonism-dementia complex of Guam. *Arch Neurol* 47:870–4

Sossi V, Doudet DJ, Holden JE (2001) A reversible tracer analysis approach to the study of effective dopamine turnover. *J Cereb Blood Flow Metab* 21:469–76

Sossi V, de La Fuente-Fernández R, Holden JE, Doudet DJ, McKenzie J, Stoessl AJ, Ruth TJ (2002) Increase in dopamine turnover occurs early in Parkinson's disease:

evidence from a new modeling approach to PET 18 F-fluorodopa data. *J Cereb Blood Flow Metab* 22:232–9

Sossi V, Holden JE, de la Fuente-Fernández R, Ruth TJ, Stoessl AJ (2003) Effect of dopamine loss and the metabolite 3-*O*-methyl-[^{18}F]fluoro-dopa on the relation between the ^{18}F-fluorodopa tissue input uptake rate constant K_{occ} and the [^{18}F]fluorodopa plasma input uptake rate constant Ki. *J Cereb Blood Flow Metab* 23:301–9

Sossi V, de la Funente-Fernández R, Holden JE, Schulzer M, Ruth TJ, Stoessl J (2004) Changes of dopamine turnover in the progression of Parkinson's disease as measured by positron emission tomography: their relation to disease-compensatory mechanisms. *J Cereb Blood Flow Metab* 24:869–76

Taylor SF, Koeppe RA, Tandon R, Zubieta JK, Frey KA (2000) *In vivo* measurement of the vesicular monoamine transporter in schizophrenia. *Neuropsychopharmacology* 23:667–75

Vingerhoets FJ, Schulzer M, Ruth TJ, Holden JE, Snow BJ (1996) Reproducibility and discriminating ability of fluorine-18-6-fluoro-L-Dopa PET in Parkinson's disease. *J Nucl Med* 37:421–6

Wahl L, Chirakal R, Firnau G, Garnett ES, Nahmias C (1994) The distribution and kinetics of [^{18}F]fluoro-*O*-methyl-L-dopa in the human brain. *J Cereb Blood Flow Metab* 14:664–70

Woods RP, Cherry SR, Mazziotta JC (1992) Rapid automated algorithm for aligning and reslicing PET images. *J Comput Assist Tomogr* 16:620–33

Yee RE, Cheng DW, Huang SC, Namavari M, Satyamurthy N, Barrio JR (2001) Blood–brain barrier and neuronal membrane transport of 6-[^{18}F]fluoro-L-DOPA. *Biochem Pharmacol* 62:1409–15